



# An apparatus for measuring water content of unsaturated soil based on the van der Pauw principle

Zhihao Yang<sup>1,2</sup> · Zurun Yue<sup>1</sup> · Tiecheng Sun<sup>1</sup> · Leiqiang Miao<sup>3</sup>

Received: 19 July 2019 / Accepted: 24 February 2020 / Published online: 9 March 2020  
© Saudi Society for Geosciences 2020

## Abstract

Understanding water migration in soil specimens under triaxial test conditions is of great significance for investigating the mechanism of distress in railway subgrades. However, the water content distribution along the specimen height is difficult to determine with current equipment. Motivated by such limitations, we developed an apparatus relying on the van der Pauw principle, to measure the water content based on the specimen's electrical properties. Additionally, a series of exploratory tests on unsaturated soil specimens were conducted to evaluate the performance of this apparatus. To verify the practicability of the apparatus, a water-supply dynamic triaxial test was also carried out with an unsaturated dynamic triaxial test system (GDS). The results indicate that this apparatus is stable, as the measurement accuracy is not influenced by the electrode position or the soil geometry or dimensions. In a narrow triaxial pressure chamber, this apparatus can be used to determine the distribution of water content in unsaturated specimens nondestructively and consecutively during a triaxial test. The maximum error obtained from the apparatus when measuring the gravimetric water content was 0.7%. The soil resistivity calculation function was obtained considering the dry density and gravimetric water content with high correlation and precision. This apparatus has broad applications for investigating the mechanism of water migration within some geotechnical materials.

**Keywords** van der Pauw principle · Unsaturated soil · Water content · Real-time measurement

## Introduction

Currently, the application of geophysics to solve engineering and environmental problems has become a research hotspot with the development of interdisciplinary research (Alabi et al. 2018; Abdellaoui et al. 2019). Analysis of soil resistivity is also an important branch of this interdisciplinary field (Liu et al. 2004). Measuring resistivity has significant advantages in studying soil physical characteristics and intelligent

monitoring (Wychowaniak et al. 2015; Rakorenko and Korotchen 2016; Han et al. 2006). The research basis is that there is a certain correlation between the research target parameter and soil resistivity. Due to the temporal and spatial complexity of geotechnical materials, their resistivity measurement is affected by a variety of factors (Archie 1942; Corwin and Lesch 2005), such as the water content, saturation, internal ion species, and concentration. Many scholars have studied the variation properties of physical parameters by the resistivity method, such as the crystal structure, water content, porosity, relative compaction, and liquid-plastic limit of soil specimens (Lee et al. 2011; Kibria and Hossain 2012; Abidin et al. 2014; Zhou et al. 2015). In the field of microcosmic research (Yu and Liu 2004), because the soil microcosmic internal structure has a direct correspondence with its macroscopic resistivity, some scholars have also used the resistivity method to study the changes of the soil microcosmic structure by quantitatively obtaining the soil matrix suction and soil-water characteristic curve based on the resistivity method (Zha et al. 2008; Zha et al. 2010).

The measurement of soil resistivity was initially carried out using the two-electrode method (ASTM 2012; Islam et al.

---

Responsible Editor: Zeynal Abiddin Erguler

✉ Zurun Yue  
731191861@qq.com

<sup>1</sup> School of Civil Engineering, Shijiazhuang Tiedao University, Shijiazhuang 050043, China

<sup>2</sup> Key Laboratory of Roads and Railway Engineering Safety Control of Ministry of Education, Shijiazhuang Tiedao University, Shijiazhuang 050043, China

<sup>3</sup> Hebei Building Research Technology Co, Ltd, Shijiazhuang 050021, China

2012; Son et al. 2009). Copper was generally used as the electrode material, and its surface was plated with nickel to prevent polarization. The size of the electrode should be consistent with the size of the specimen's section, and the current should be evenly passed through the soil specimen (Liu et al. 2004). Later, due to the strict requirements of the two-electrode method, the four-electrode method was proposed accordingly. In the four-electrode method, two electrodes apply a current, and the other two electrodes are used to measure the resulting voltage drop to calculate the resistivity of the specimen. When the distance between the four electrodes is equal, it is called the Wenner configuration (Zhou and Lee 2010). Otherwise, when the distance is arbitrary, it is called Schlumberger configuration (Burger and Burger 1992). Although the above two methods are different in principle, both require full contact between the electrode and the soil, which is difficult to ensure in practical engineering operation, resulting in errors in the measurement. The limitation of current research is that the test accuracy is not high. The error is sometimes more than 5%. With the development of test technology, the test requirements are becoming increasingly higher. In many cases, it is required not to destruct the specimen while measuring its resistivity, so that other physical and mechanical properties of the specimen can be measured subsequently. Nondestructive and time testing technology for soil resistivity has received increasing interest (Zhou et al. 2009).

The van der Pauw method (Muno-zcastelblanco et al. 2013; Preis 2015) is a method to measure the resistivity of electrolyte solutions and electronic materials. In this method, the electrodes are arranged around the specimen. The specimen can be of any shape with a uniform thickness, which is the result of theoretical derivation in combination with the van der Pauw theory and the conformal mapping theory in the field of electricity (Vander 1958). Many scholars have conducted research on the electrical working mechanism and testing principle of the van der Pauw method (Nahlik et al. 2013; Banaszczyk et al. 2010), and their results indicate that this method is very reliable. As long as the resistance of the tested electrode is small enough relative to the specimen, the influence of the electrode shape on the test can be ignored (Nahlik et al. 2011). In the conventional method, the electrodes need to be inserted into the interior of the soil sample, so it is challenging to ensure full contact between the test electrode and the soil sample. In the van der Pauw method, the electrodes must be placed around the soil sample. Due to the good ductility of the electrodes and good elasticity of the rubber membrane, it is easy to ensure effective contact between the electrodes and the soil samples.

This paper introduces the van der Pauw method to the field of geotechnical testing. A test apparatus was developed, and the effectiveness of this apparatus was studied. In addition, the test unit of the device is embedded in the dynamic triaxial apparatus, and an effective sealing connection is realized

between the test unit inside the confining pressure chamber and the collecting device outside the chamber. In addition, we conducted a water-supply dynamic triaxial test combined with a dynamic triaxial test apparatus (GDS). For the first time, the continuous measurement of the water content distribution along the height of the specimen during a triaxial test is realized. This apparatus overcomes the limitation of the current testing equipment and provides a feasible means for geotechnical engineering to perform nondestructive and simultaneous water-force property testing of soil under dynamic loading. Moreover, this method is expected to provide a feasible means for exploring the water migration mechanism of many geotechnical problems, such as mud-pumping, frost heave and thawing, and loess collapsibility.

## Methodology

The apparatus is based on the van der Pauw principle (Moron 2003; Grysinski and Moron 2011), and the measurement setup is illustrated in Fig. 1. Four electrodes are arranged around the specimen, and the current is input and output from the two ends. An electric field is generated inside the specimen, and the corresponding voltage is generated between the other two ends. The resistance is obtained by dividing the voltage by the current. The test is carried out in two steps. First, NO are used as the current terminals, MP are used as the voltage test terminals, and the resistance  $R_{NO,MP}$  is calculated. Second, PO are used as the current terminals, MN are used as the voltage test terminals, and the resistance  $R_{PO,MN}$  is calculated. The corresponding resistivity  $\rho$  of the specimen can be evaluated by the van der Pauw formula (Grysinski and Moron 2011).

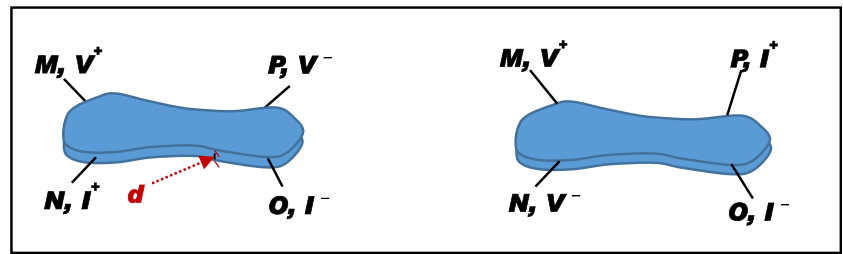
$$\exp\left(\frac{\pi d R_{NO,MP}}{\rho}\right) + \exp\left(-\frac{\pi d R_{PO,MN}}{\rho}\right) = 1 \quad (1)$$

where  $\pi$  is a mathematical constant, 3.14;  $\rho$  is the specimen resistivity; and  $d$  is the specimen thickness. When  $R_{NO,MP}$  and  $R_{PO,MN}$  are equal, we can obtain an analytic solution for  $\rho$ . In most cases,  $R_{NO,MP}$  is not equal to  $R_{PO,MN}$ , and the bisection algorithm or Newton iteration method can be adopted to solve the problem. These two methods are efficient ways to find approximate solutions to equations with arbitrary accuracy. Because the Newton iteration method has a better iteration efficiency, the authors adopted the Newton iteration method in this experiment.

## Test apparatus

The test apparatus mainly includes test electrodes, a constant current source that can input a constant AC current to the soil specimen, an electrode controller, a signal acquisition instrument, and a computer.

**Fig. 1** Electrode layout of the test principle



(a) *NO* are the input and output current terminals (b) *PO* are the input and output current terminals

After comprehensive material comparison and selection in the test, titanium with its good antipolarization and conductive properties is selected as the electrode material. The length and width of each electrode are 10 mm and 5 mm, respectively. The thickness is 0.02 mm. Due to the material characteristics of titanium, it is impossible to use solder to metallurgically bond the titanium-platinum sheet and the wire. Because of the good electrical conductivity and ductility of the copper foil, the copper foil is cut into fine sheets, and the length and width of each sheet are approximately 0.2 mm and 0.1 mm, respectively. Then, the copper sheet is pressed on the edge of the titanium-platinum sheet. In addition, the wire is placed between the copper sheet and the titanium-platinum sheet to realize the contact between the titanium-platinum sheet and the wire. The four electrodes are fixed on the rubber membrane with glue according to the designed position of the different test content. At the same time, a measurement unit is obtained and placed around the specimen. We intentionally increased the tightness of the rubber membrane when preparing the specimen. Even if the specimen deforms during the dynamic triaxial test, the elasticity of the rubber membrane can ensure full contact between the test electrode and the soil. The arrangement of the test electrode on the rubber membrane is shown in Fig. 2. The contact between the soil and the electrode is shown in Fig. 3.

Although there are many ions in the specimen, the polarization phenomenon caused by the directional movement of ions can be effectively prevented by selecting the AC source as the current input source. The constant current source used in this apparatus can output a constant ac current between 0~1 mA, and the output waveform is a sine wave with a frequency range of 100~1000 Hz. Switching of the input current and tested voltage electrode can be realized by an electrode controller. The equipment for measuring voltage is the Agilent Technologies E8084A which has 64 channels. The acquisition frequency is 20 MHz, and the precision is 0.001. This tool has the advantages of high precision, low distortion, low noise, good channel consistency, and good matching performance. The built-in VT1436 VXI module has a scanning speed of 51.2 k specimens /sec/channel, as well as the optional voltage, charge, microphone, or IEPE input signal modes, which can realize the simultaneous acquisition of data on nodes 64 to 8192. IEPE refers to an accelerometer with its own power amplifier or voltage amplifier.

The automatic calculation software is programmed independently, to automatically calculate and store the specimen resistivity according to the collected voltage and the set current in the test process. The flow chart of the test system is shown in Fig. 4.

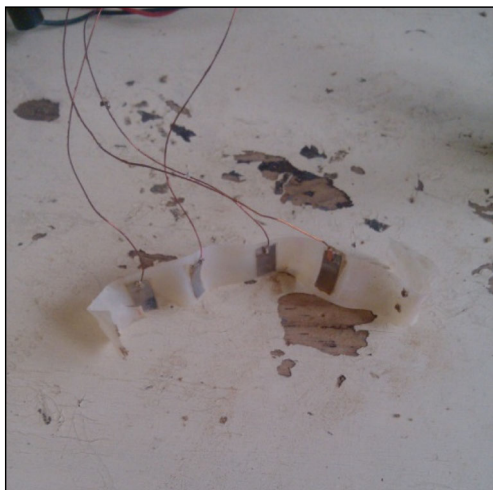


**Fig. 2** The electrode layout on the rubber membrane

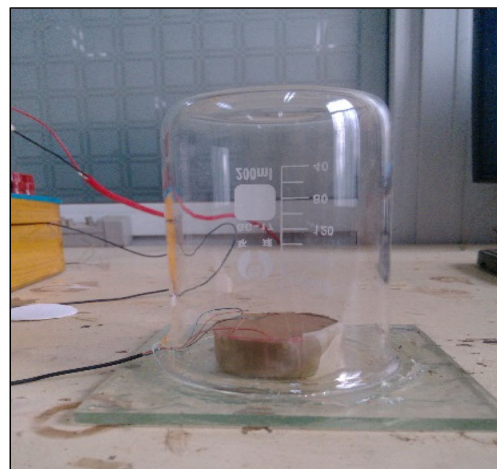


**Fig. 3** Verification of the measurement sensitivity over time

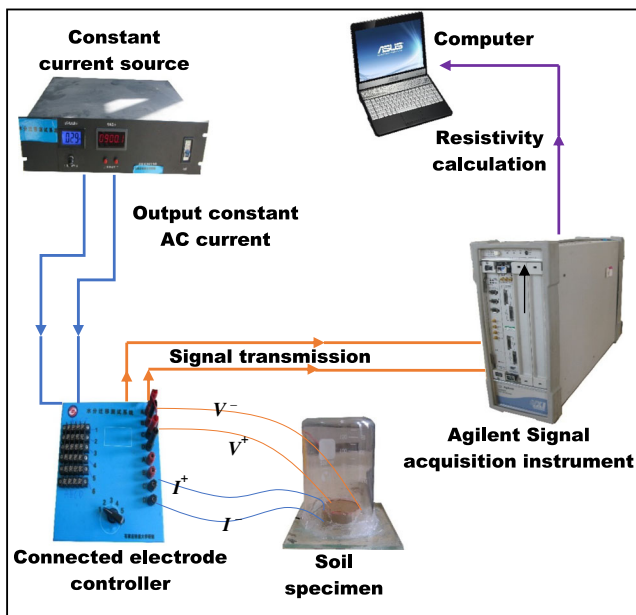


Fig. 4 Test apparatus

## Experimental design

### Physical properties of tested soil specimens

The soil was taken from a typical section of subgrade with pumping in the Shuo Huang railway, with a specific gravity of 2.65, a liquid limit of 26%, a plastic limit of 16%, an optimal moisture content of 14.4%, and a maximum dry density of  $1.92 \text{ g cm}^{-3}$ . According to China railway engineering geotechnical test code TB10102-2010, the soil specimen was defined as silt. The dry density and gravimetric water content involved in this paper are all for roadbed filling. The designed range of dry density was determined by the in situ test on the roadbed filling. The designed range of gravimetric water content was below the saturated moisture content of roadbed filling.

### Sensitivity of the test apparatus

#### (a) Effect of foreign ions

To limit the impact of salt, the method of soil washing was adopted to desalinate the soil sample. When washing the soil, the operator's hands should first be washed with pure water. The protocol is as follows. First, remove the impurities from the test soil and place them in the basin. Then pour the water, infiltrate for 2 h, stir by hand to an earth-like consistency, and then let it stand. After the soil particles are fully precipitated, the upper water is poured out, and finally, the soil sample is dried, crushed, and prepared. Washing the soil several times requires repeating the above steps. Pure water was used as the water sample. For each soil washing step, an appropriate

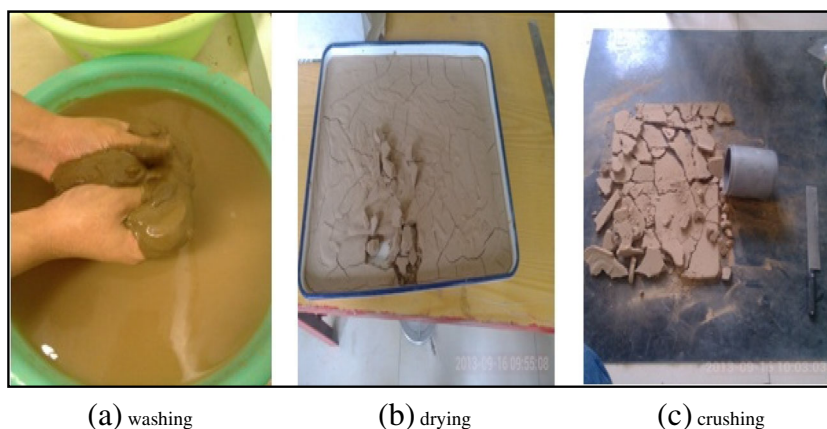
amount of soil was dried to prepare soil specimens with a gravimetric water content of 10% and a dry density of  $1.79 \text{ g cm}^{-3}$ . These specimens were used in the resistivity measurement. Three parallel tests were performed in each test in which the soil was washed specified times, and then the values were averaged. We repeated resistivity measurement tests with various times of soil washing and drew relationships between soil resistivity and times of soil washing. We performed soil washing as much as possible and eliminated errors from free ions in the original soil samples to provide a basis for calibration experiments. Figure 5 demonstrates the soil washing processes.

#### (b) Effect of electrode placement

To avoid measurement error caused by differences in the electrode positions which are arranged manually, an electrode position verification test was carried out. Soil specimens with a gravimetric water content of 10%, a dry density of  $1.82 \text{ g cm}^{-3}$ , a diameter of 39.1 mm and a height of 10 mm were selected. The soil sample that has not been washed was selected. Bottled mineral water was used for preparing the soil with a specific gravimetric water content. The electrodes were arranged as shown in Fig. 6. The two electrodes B and E are located on the plane diameter line of the soil specimen and are symmetrically attached to the side surface of the soil sample. The two electrodes C and D are adhered to the side surface of the semicircular soil specimen on one side of the BE diameter line and are at an angle of  $60^\circ$  with the angle of the BE line. The A electrode is closely attached at an intermediate position on the side surface of the semicircular soil specimen on the other side of the BE diameter line. The selected five electrode positions can fully cover the differences in the artificial arrangement of the electrode positions, and the influence of the verification electrode position on the resistivity test is representative. Since electrodes C and D are equivalent and the electrodes B and E are equivalent, the electrode connection test was conducted in three cases (ACDE, BCDE, and ABDE), and five sets of parallel tests were conducted in each case to analyze the test results.

Multiple time points were selected to measure the resistivity of the same specimen to verify the dynamic response of the test apparatus. To prevent error caused by the loss of gravimetric water content during the test, the soil specimen was sealed and covered with a beaker. Vaseline was daubed around the specimen, and the soil specimen was maintained in a static and non-energized state, as shown in Fig. 3.

**Fig. 5** Selected portions of the test process of washing the soil



(c) Influence of the specimen geometry.

The research of this test apparatus mainly involves the dynamic measurement of the layered gravimetric water content of the specimen during the triaxial test. However, the soil specimen will inevitably deform during the test, and whether the measured resistivity value of the deformed specimen remains accurate needs to be verified. Therefore, the standard specimen with a diameter of 39.1 mm was cut into three different shapes as shown in Fig. 7 for resistivity measurement. The three shapes represent the common deformation modes of the specimens under different stress levels and working conditions during the triaxial test. They are divided into normal stable specimen A with a diameter of 19.5 mm, elliptical irregular deformation specimen B with a long-axis diameter of 25.23 mm, and standard triaxial transverse deformation specimen C with a diameter of 25.23 mm. The specimens all had a dry density of  $1.82 \text{ g cm}^{-3}$  and a gravimetric water content of 9%. The soil sample that has not been washed was selected. Bottled mineral water was used

for preparing the soil with a specific gravimetric water content. Five parallel tests were conducted, and the test results were analyzed.

(d) Effect of the specimen height

To verify whether a change in the height of the triaxial specimen has an effect on the results, a resistivity measurement test under two height conditions was carried out. The soil sample that has not been washed was selected. Bottled mineral water was used for preparing the soil with a specific gravimetric water content.

The specimen was arranged with 8 layered electrodes at different heights as shown in Fig. 8. The gravimetric water content, dry density, diameter, and height of the specimen are 10%,  $1.82 \text{ g cm}^{-3}$ , 39.1 mm, and 80 mm, respectively. After the soil specimen was arranged with a static seal and not energized for 24 h, the resistivity was measured.

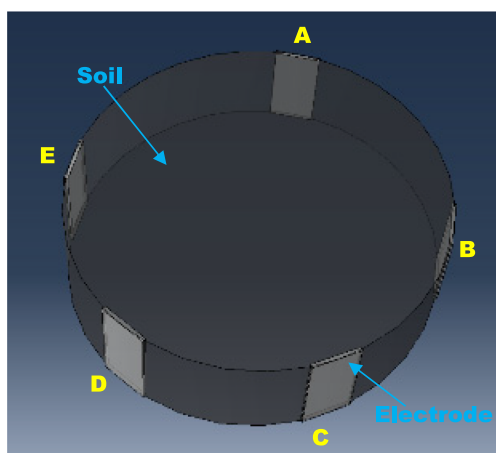


**Fig. 6** The measurement of the resistivity with different connected electrodes

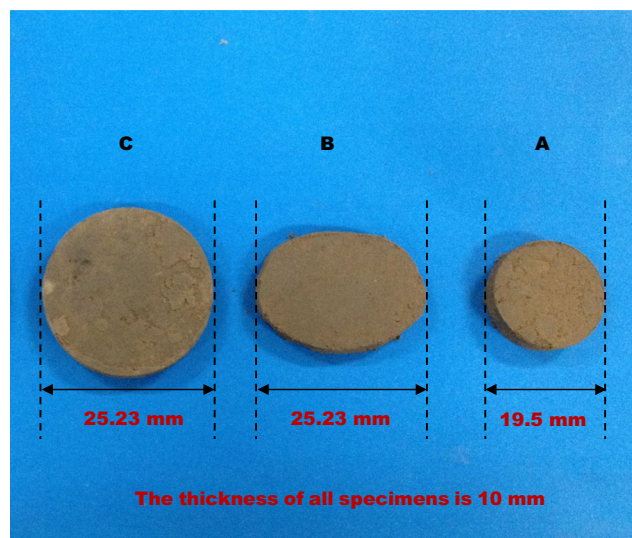


**Fig. 7** Resistivity measurement with different shapes



**Fig. 8** Calibration in the direction of height

Soil specimens of different heights (10 mm, 20 mm, 30 mm, 40 mm, 60 mm, 80 mm) were prepared. The electrodes were arranged on top of each specimen with a static seal and non-energized for 24 h, and then the resistivity was measured.

(e) Effect of the metal component

In the triaxial test, soil specimens need to be placed on the lower metal column. To verify whether the metal column affects the distribution of the electric field inside the specimen, a resistivity measurement test of the specimen with a metal component on the bottom was conducted, as shown in Fig. 9. The specimen diameter and height are 39.1 mm and 30 mm, respectively. The soil sample that has not been washed was selected. Bottled mineral water was used for preparing the soil with a specific gravimetric water content. Five specimens were prepared for the test. Since the purpose was to test the influence of the metal component on the test results, the dry density and gravimetric water content were not strictly regulated when preparing the specimens. All samples were prepared and selected randomly for testing.

(f) Effect of the solute concentration

To increase the effect of the water content on the resistivity, pure water was replaced with a salt solution during the preparation of soil samples. Through

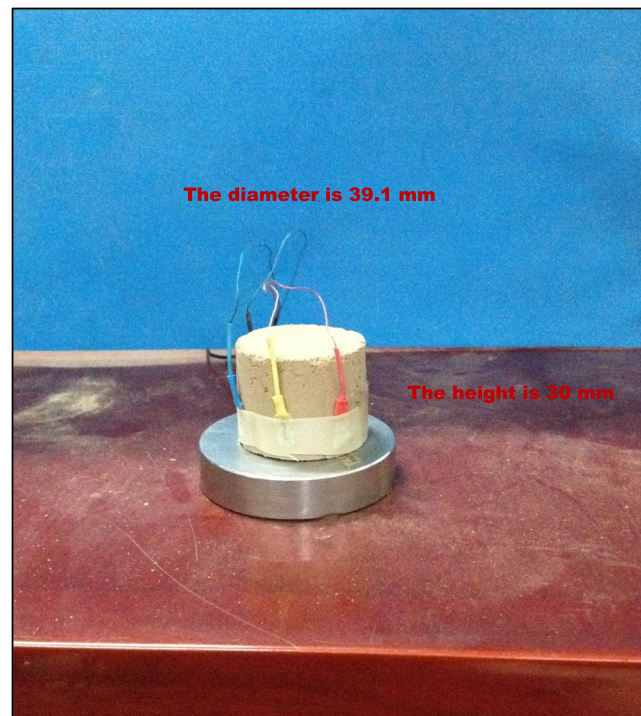


**Fig. 9** Resistivity measurement with a metal seat

comparison and analysis,  $\text{Na}_2\text{SO}_4$  was selected as the test solute. We configured  $\text{Na}_2\text{SO}_4$  solutions with a concentration of 0%, 3%, 5%, 7%, 9%, 12%, and 15% to prepare soil samples with a gravimetric water content of 10% and a dry density of  $1.82 \text{ g cm}^{-3}$ . The soil sample that has been washed 8 times was selected. We aimed to obtain the precise solution affecting the test results, improve the accuracy of the test, and provide a basis for follow-up tests.

### Effect of the gravimetric water content and dry density

To meet the experimental requirements of simulating sub-grade deformation under different dry density in the process of triaxial testing, the cross test on resistivity measurements were carried out. These experiments were also conducted after the verification test on the stability and influence factors of the apparatus had completed. The relationship between the gravimetric water content, dry density, and resistivity was explored according to the soil specimens with different dry density levels ( $1.65 \text{ g cm}^{-3}$ ,  $1.71 \text{ g cm}^{-3}$ ,  $1.75 \text{ g cm}^{-3}$ ,  $1.79 \text{ g cm}^{-3}$ ) and different gravimetric water contents (5%, 6%, 8%, 10%, 12%, 14%, 16%, 18%, 20%, 22%, 24%). The soil sample that has been washed 8 times was selected. The optimal water content was 14.4%, and the maximum dry density was  $1.92 \text{ g cm}^{-3}$ . The diameter and height of the soil specimens were 39.1 mm and 10 mm respectively.

## Verification test

To verify the accuracy of the test device, a verification test was designed. The gravimetric water content values, which were measured by the van der Pauw method and the conventional drying method were analyzed. The soil specimens with a designed gravimetric water content (12%, 14%, 16%, 18%) and a dry density of  $1.79 \text{ g}\cdot\text{cm}^{-3}$  were prepared. The error between the gravimetric water content by the conventional method and the gravimetric water content obtained from the apparatus was calculated to verify the accuracy of the calibration function.

## Consecutive measurement on layered gravimetric water content of the specimens in the water-supply dynamic triaxial test

To verify the practicability of this apparatus, a water-supply dynamic triaxial test was carried out with the GDS. Combined with the independently developed Martens flask device, the water supply of the specimen was conducted in the process of cyclic triaxial test through the reserved confining pressure hole of the cyclic triaxial instrument, simulating the actual working conditions of subgrade under the combined action of cyclic load and rainfall. To explore the feasibility of testing the internal water migration of specimens with this apparatus, the layered gravimetric water content of the soil specimens was continuously measured during the test.

Soil specimens with a dry density of  $1.71 \text{ g}\cdot\text{cm}^{-3}$  and a gravimetric water content of 10% were prepared to conduct the water-supply dynamic triaxial test with a confining pressure of 30 kPa and a dynamic stress amplitude of 30 kPa. Soil specimens with dry density levels of  $1.65 \text{ g}\cdot\text{cm}^{-3}$ ,  $1.71 \text{ g}\cdot\text{cm}^{-3}$ ,  $1.75 \text{ g}\cdot\text{cm}^{-3}$ , and  $1.79 \text{ g}\cdot\text{cm}^{-3}$  and a gravimetric water content of 10% were prepared to conduct this test with a confining pressure of 30 kPa and dynamic stress amplitude of 90 kPa. All parameters in the water-supply dynamic triaxial test were designed in combination with the actual field engineering to simulate the actual working conditions at the site. All specimens' diameters and heights were 39.1 mm and 80 mm, respectively. The test loading frequency was 1 Hz, and the loading waveform was a sine wave. The number of cyclic loading steps of the axial load during this test was 3600.

The difficulty in this test is how to ensure that the measurement electrode arranged around the specimens is connected with the data acquisition device outside of the confining pressure chamber, and how to seal the pressure chamber to prevent water leakage during the test. To solve this problem, we modified the reserve hole for confining pressure in the lower part of the confining pressure chamber of the GDS, as shown in Fig. 10. In addition, a threaded connector and O-ring for the reserved hole size were specially developed. Additionally, we ran the wire through a heat-shrinkable tube and used a syringe to inject the liquid silica gel with coagulant into the heat-

shrinkable tube. A hot air gun was then used to supply heating until the silica gel was extruded from the heat-shrinkable tube. After the liquid silica gel condensed into solid silica gel, we transferred the heat-shrinkable tube filled with wire and silica gel to the nut end of the tube and screwed the nut on the screw to achieve the sealing effect. The sealing effect of this method was confirmed to be suitable, with no water leakage observed up to a confining pressure of at least 500 kPa.

## Results

### Effect of soil washing

The resistivity of soil samples in certain gravimetric water contents and dry density varies with increasing of soil washing times. The testing variation curve is shown in Fig. 11.

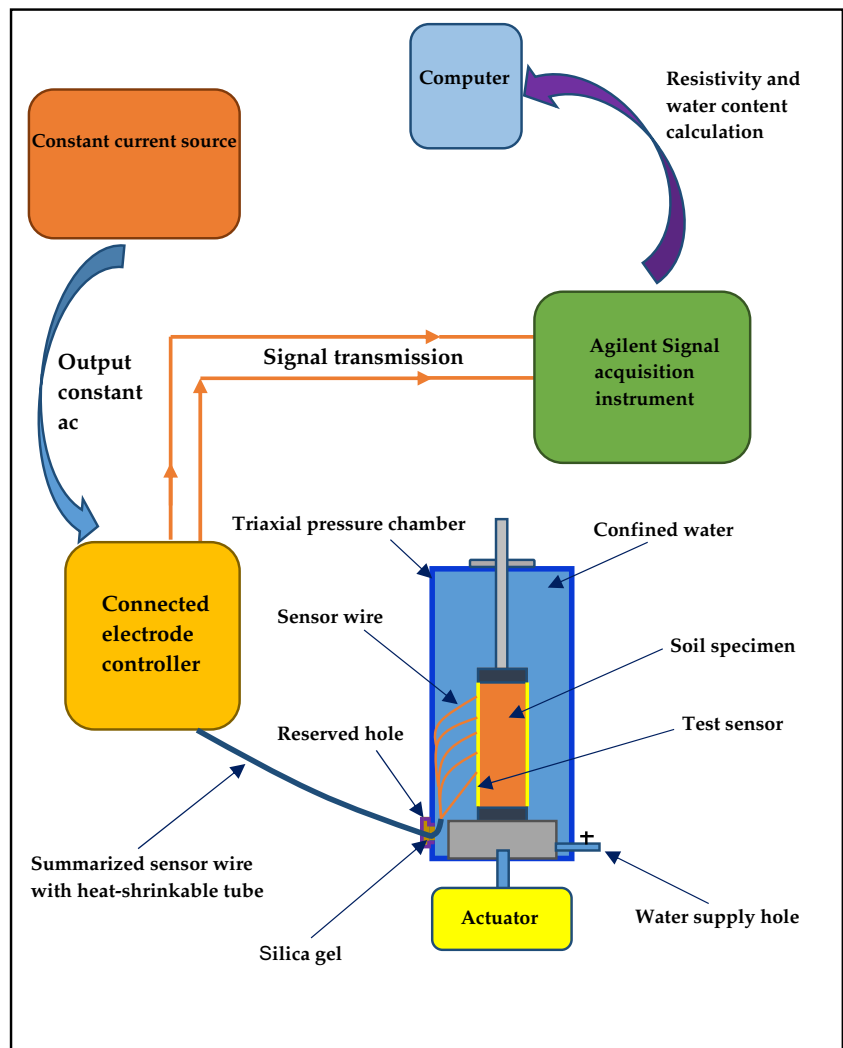
We can conclude from Fig. 11 that soil resistivity increases with increasing soil washing times. The rate of increase is high at the initial stage and subsequently slows down because free impurity ions are highly soluble in the rinse water, decreasing the number of free ions. The maximum standard deviation of each repeated test is 0.97. The value of resistivity is the same when the soil washing time is 6 and 7, from which we can conclude that soil with 6 washing times reaches the goal of eliminating internal impurity ions. To improve accuracy, the soil was washed 8 times in the calibration test for resistivity, gravimetric water content, and dry density.

### Effect of the electrode position difference

Figure 12 shows the variation trend of resistivity with time in three cases of different connected electrodes. Combined with the test results, the stability of the apparatus over time could be explored.

Because the temperature of the laboratory does not change much during the relevant tests, the influence of the temperature change of the laboratory on the resistivity test is small compared with the influence of the gravimetric water content on the resistivity test. So we can think that the effect of temperature on resistivity is negligible. The maximum error in resistivity in the test of three-electrode placement is  $6 \Omega \cdot \text{m}$ . The maximum change over time is  $4 \Omega \cdot \text{m}$ . From the later-derived calibration function between the resistivity and gravimetric water content, it can be seen that the error in the calculated gravimetric water content with the different electrode positions meets the Chinese standard requirements for an allowable error of 1% in the field of civil engineering. The error is caused by the uneven distribution of gravimetric water content in the preparation of the soil specimens, which is a systematic error. The results indicate that the difference in electrode position has little effect on the resistivity measurement and that the apparatus has good stability and accuracy.

**Fig. 10** Schematic diagram of the water content test apparatus connected to the dynamic triaxial instrument



**Effect of the specimen geometry**

The measurement results on the resistivity of soil specimens with different geometric shapes under the same dry density and gravimetric water content are shown in Table. 1.

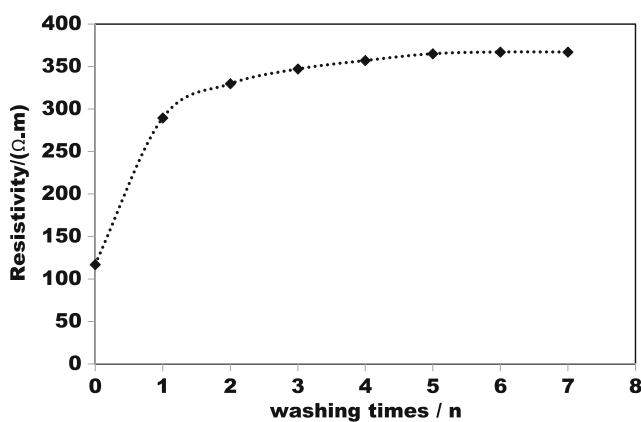


**Fig. 11** Resistivity vs washing times

Table 1 shows that the maximum resistivity error of the soil specimens with four different geometric shapes is 1.08%. The error in the gravimetric water content as obtained by the reverse calculation is less than 1%, which meets the requirements of the specification. The results show that the specimen

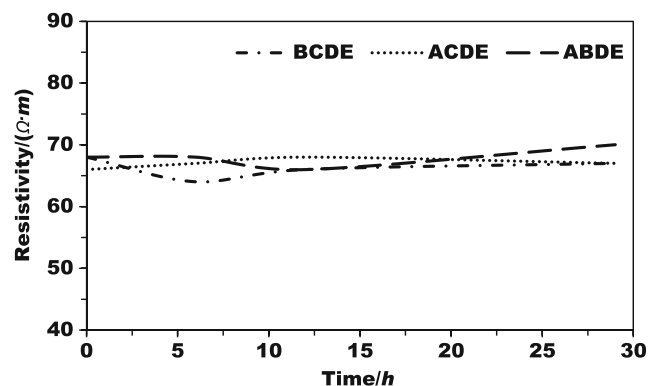


**Fig. 12** Resistivity vs time with electrode layout differences



**Table 1** Resistivity of specimens with different geometrical shapes

Geometrical shape	Cylindrical		Elliptically cylindrical
	$r = 19.5 \text{ mm}$	$r = 25.23 \text{ mm}$	
Resistivity/( $\Omega \text{ m}$ )	90	91	92

resistivity does not change after the specimen is deformed in the triaxial test, and the gravimetric water content of soil specimens can still be measured precisely.

**Effect of metal parts**

The resistivity of five soil specimens was tested with or without metal parts on the bottom of the specimen. The tested results are shown in Fig. 13.

The maximum resistivity error of the five soil specimens for no metal member and a metal member in the end portion is  $6 \Omega \text{ m}$ , and the maximum standard deviation of each repeated test is 0.99, showing that the metal parts have no effect on the determination of the specimen gravimetric water content during the triaxial test.

**Effect of the solution concentration of  $\text{Na}_2\text{SO}_4$**

As a strong electrolyte, a  $\text{Na}_2\text{SO}_4$  solution was used to configure soil samples, which is expected to have an obvious effect and to present a large change trend. The influence relation curve is shown in Fig. 14.

The maximum standard deviation of each repeated test is 0.96. From Fig. 14, we can see that, in general, the resistivity decreases with increasing concentration, and the decreasing trend is significant from 0 to 7% and almost linear. Subsequently, the resistivity decreases slowly with increasing concentration in general, but we can see fluctuation of the curve at a concentration of 9%. For strong electrolytes, such as  $\text{Na}_2\text{SO}_4$  solution, the resistivity decreases clearly with increasing concentration because of the increase in ion

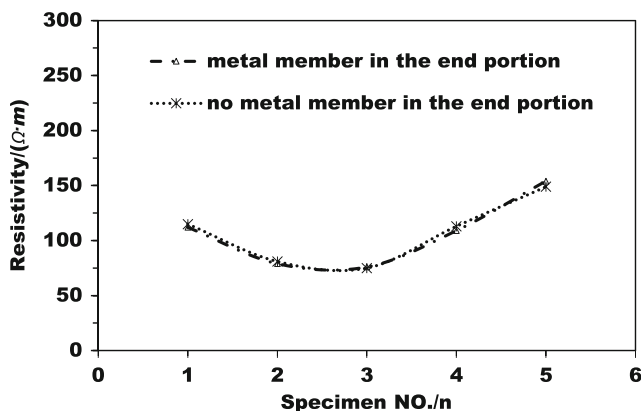


**Fig. 13** Calibration curve of resistivity measurement with a metal seat

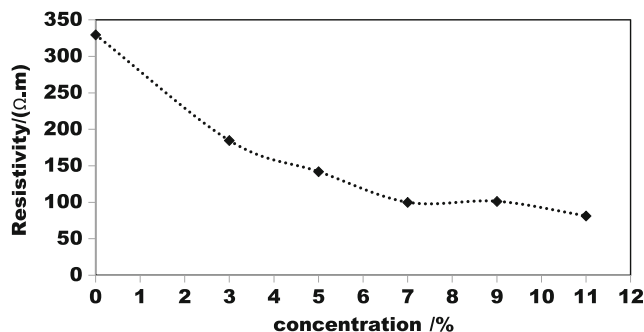


**Fig. 14** The effect of solution concentration by weight on the resistivity

concentration in the unit volume solution when the soil is not washed to remove them. Moreover, the interaction force between  $\text{Na}^+$  and  $\text{SO}_4^{2-}$  increases with increasing concentration and thus affects the conductive property. After the concentration exceeds a certain value, the influence on the decrease in conduction caused by interaction forces is larger than the effect on the increase in conduction resulting from the increase in ionic concentration. At this time, the resistivity decreases with increasing concentration, and then another inflection point appears in the calibration curve of the concentration and conductivity.

**Effect of the specimen height**

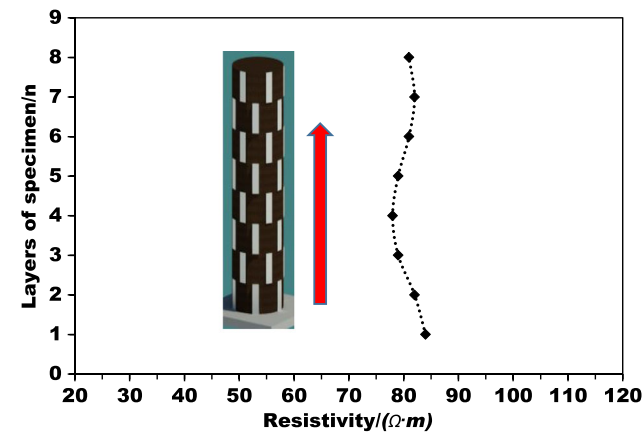
Figure 15 a shows the resistivity measurements along the height of the same specimen. The results of resistivity measurement at the top of soil specimens with different heights (10 mm, 20 mm, 30 mm, 40 mm, 60 mm, and 80 mm) are shown in Fig. 15b.

For the same specimen, the maximum error in resistivity measured at different heights is  $6 \Omega \text{ m}$ . The maximum tested resistivity error of the specimens with different heights is  $7 \Omega \text{ m}$ . Both are within the error range of the specification requirements. The layered gravimetric water content of the specimen at different heights during the triaxial test can be measured, and the multiple channels do not interfere with each other. When we conducted the calibration test of the resistivity and gravimetric water content, the calibration of specimens with a single height was found to be sufficient. At this time, the calibration function is also applicable to soil specimens with other heights.

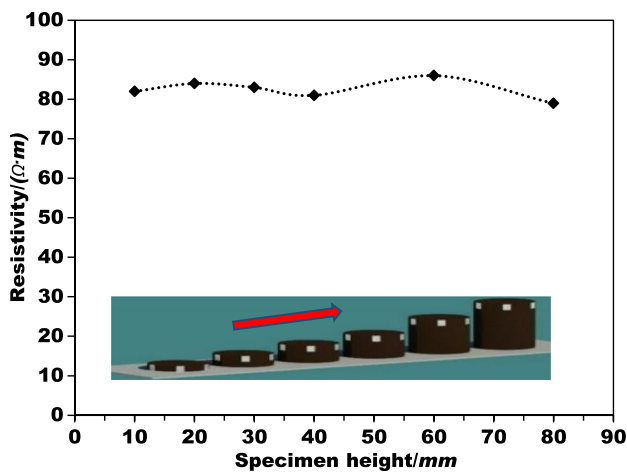
**Relationship between the resistivity and gravimetric water content, dry density**

The tested resistivities of specimens with different dry density and gravimetric water content are shown in Fig. 16.

As a whole, as the gravimetric water content increases, the resistivity decreases gradually and the change trend gradually decreases. As the gravimetric water content increases, the number of ions in the unit volume of the soil sample increases



(a) Resistivity measurement at different heights in the same specimen



(b) Resistivity measurement at the same location of specimens with different heights

Fig. 15 Resistivity vs specimen height

strongly, so the resistivity decreases strongly. When the gravimetric water content is close to the saturated water content, the pores between the particles are completely penetrated by water, and the current is transmitted mainly through the interparticle water channel. As the gravimetric water content continues to increase, the path through which the current passes

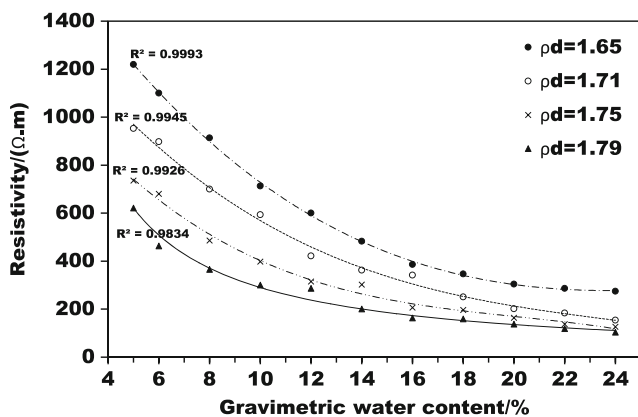


Fig. 16 Resistivity vs gravimetric water content with different dry density

is unchanged, so the resistivity does not change much. As the dry density increases, the resistivity decreases successively. Because the dry density increases, the pores between the particles decrease, the pores penetrated by water molecules decrease under the same gravimetric water content, and the resistivity decreases. As the gravimetric water content increases, the influence degree of dry density on the resistivity becomes weaker, and when the gravimetric water content reaches the saturated water content, the dry density has little effect on the resistivity. As the gravimetric water content increases, the current dominates through the water channel path between the particles, and the change in resistivity caused by the solid-liquid channel and the solid-solid channel path caused by the increase in dry density is relatively small. An exponential or power function relationship can be fit between the gravimetric water content of the soil sample and its resistivity (Singh 2004), and an exponential or power function relationship can also be fitted between the resistivity and the relative compaction (Ferre et al. 1998). In this paper, a comprehensive analysis is carried out for different fitting methods. Finally, an exponential function is selected to fit the relationship between the resistivity, dry density, and gravimetric water content. A formula for calculating the soil resistivity considering the gravimetric water content and the dry density parameter is obtained, as shown in Formula (2).

$$\rho = ae^{-b\rho_d} * e^{-cw} \tag{2}$$

where  $\rho$  is the resistivity, with units of  $\Omega$  m;  $\rho_d$  is the dry density;  $w$  is the soil gravimetric water content; and  $a$ ,  $b$ , and  $c$  are the fitting parameters related to the soil properties, which in this test are  $2.598 \text{ e}+07$ ,  $0.19079$ , and  $10.99$ , respectively.

### Verification test

Figure 17 shows the results of the gravimetric water content by the conventional method and the tested gravimetric water

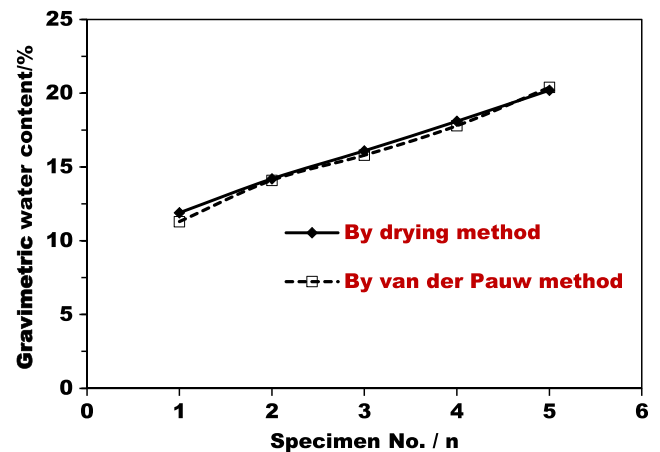


Fig. 17 Gravimetric water content vs specimen number by different methods

content by the van der Pauw method. The latter was estimated by using the calibration curve in Fig. 16. The accuracy of gravimetric water content estimation depends on several factors (the water salinity, dry density, and soil type) being the same as that when the calibration curve was obtained. The test soil was the same as in the calibration test, and it was also the soil sample after washing 8 times. Na<sub>2</sub>SO<sub>4</sub> solution of the same concentration was used to prepare a certain gravimetric water content (12%, 14%, 16%, 18%), and the dry density is 1.79 g cm<sup>-3</sup>, so as to ensure the same water salinity, dry density, and soil type. Finally, the gravimetric water content was estimated by using the calibration curve with a dry density of 1.79 g·cm<sup>-3</sup> in Fig. 17.

The maximum error between the tested gravimetric water content by the van der Pauw method and the gravimetric water content by drying method is 0.6%, and the maximum standard deviation of each repeated test is 0.95, indicating that the apparatus has a high accuracy. This work provides an effective means for the dynamic measurement of the distribution of gravimetric water content inside the specimen during a triaxial test.

### Example results from the water-supply dynamic triaxial test

The tested results of specimens' layered gravimetric water content under different test conditions are shown in Figs. 18, 19, and 20. The soil specimens were evenly divided into 8 layers with a thickness of 10 mm.

From Figs. 18 and 19, it can be seen that in the water-supply dynamic triaxial test, the gravimetric water content of the soil specimens in each layer increases linearly with time, but the growth rate is different. The gravimetric water content of the second and third layers increases significantly, and that

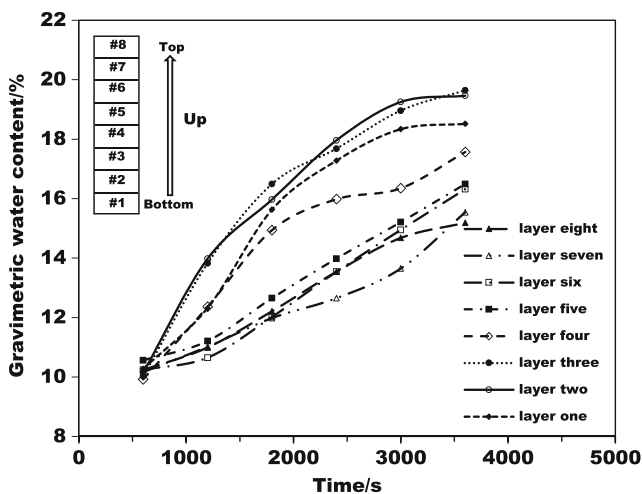


Fig. 18 Gravimetric water content vs time during the triaxial test at different layers

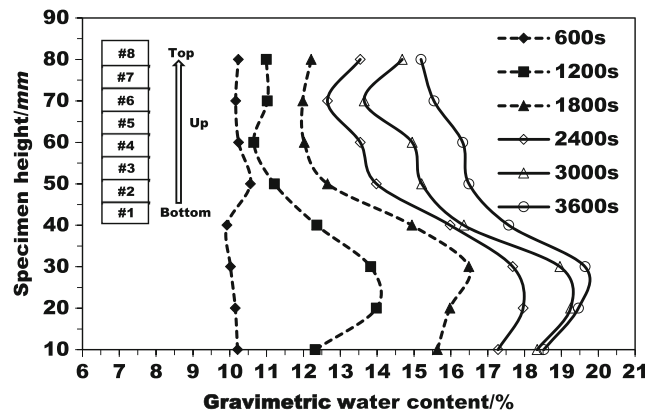


Fig. 19 Gravimetric water content vs specimen height at different time

for layers five to eight increases slowly. As seen in Fig. 20, the soil at a height of 20–30 mm area has the maximum gravimetric water content. The test results show that internal water migration occurs over the whole specimen. The gravimetric water content of the soil at a height of 20–30 mm was the maximum. The upper dynamic load generates pumping action inside the subgrade, and the potential energy to drive the internal water migration of the soil is in the opposite direction, resulting in the maximum gravimetric water content in this position under the coupling action. In addition, under the action of dynamic load, the pore water pressure rises, the strength of the soil decreases, and the deformation increases sharply, which further enhances the impact of the continuous dynamic load and increases the deformation, thereby leading to the occurrence of distress. The dynamic stress amplitude and dry density have an effect on the water migration inside the subgrade, and as the dynamic stress amplitude and dry density increase, the amount of water migration inside the specimen will decrease. It shows that increasing the dynamic stress amplitude and dry density will inhibit the water migration inside the sample.

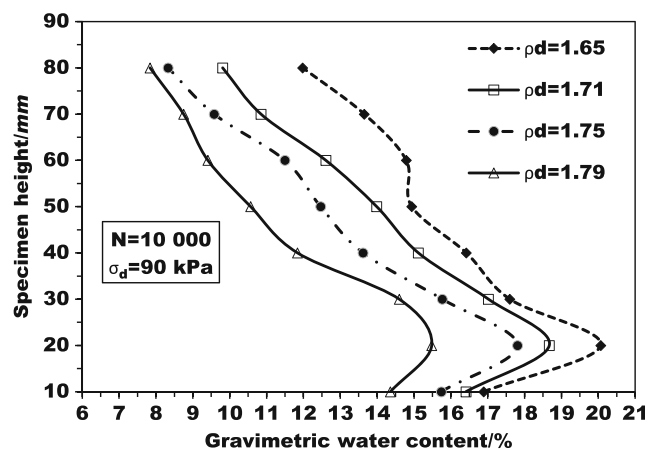


Fig. 20 Gravimetric water content vs specimen height with different dry density at the end of the triaxial test

## Conclusions

In this paper, a water content apparatus was developed based on the soil specimen's electrical properties. Additionally, a series of exploratory tests on unsaturated soil specimens were conducted to evaluate the performance of this apparatus. To verify the practicability of the apparatus, a water-supply dynamic triaxial test was also carried out with an unsaturated dynamic triaxial test system. This method can be used for determining the gravimetric water content distribution of unsaturated soil specimens along the height during a triaxial test nondestructively and simultaneously in a narrow triaxial pressure chamber.

1. This apparatus is scientifically rigorous and reasonable and has high accuracy, stability, and repeatability for the measurement of unsaturated soil specimen resistivity. The maximum measurement error in the gravimetric water content is 0.7%.
2. The test range is wide. The influence of the electrode position, the specimen geometry, the metal parts on the bottom of the specimen, and the specimen height on the accuracy and stability of the test system can be ignored.
3. The self-developed apparatus was incorporated into the water-supply dynamic triaxial test, and the results were good. This apparatus is able to dynamically measure the layered gravimetric water content of soil specimens during the triaxial test, and it is applicable to the conditions of different dry density.

**Funding information** This research was funded by the National Natural Science Foundation of China under grant no. 51178281, the Natural Science Foundation of Hebei Province under grant no. E2015210006, and the Doctoral Research Funding Project of Hebei Province under grant no. CXZZBS2017134.

## References

- Abdellaoui H, Zaourar N, Kahlouche S (2019) Contribution of permanent stations GPS data to estimate the water vapor content over Algeria. *Arab J Geosci* 12(3):81–94
- Abidin M, Saad R, Ahmad F et al (2014) Correlation analysis between field electrical resistivity value (ERV) and basic geotechnical properties (BGP). *Soil Mech Found Eng* 51(3):117–125
- Alabi A, Akinyemi O, Olowofela J et al (2018) Estimation of ground water content using water balance and regression approach. *Arab J Geosci* 11(21):659–674
- Archie G (1942) Electrical resistivity an aid in core-analysis interpretation. *AAPG Bull Am Assoc Pet Geol* 31(2):350–366
- ASTM (2012) G57-06-2012. America society for testing and materials, standard test method for field measurement of soil resistivity using the WENNER four-electrode method[S].
- Banaszczyk J, Schwarz A, Mey G et al (2010) The Vander Pauw method for sheet resistance measurements of polypyrrole-coated para-aramide woven fabrics. *J Appl Polym Sci* 117(5):2553–2558
- Burger H, Burger D (1992) Exploration geophysics of the shallow subsurface[M]. Upper Saddle River, Prentice Hall
- Corwin D, Lesch S (2005) Apparent soil electrical conductivity measurements in agriculture. *Comput Electron Agric* 46(1/2/3):11–43
- Ferre P, Redman J, Rudolph D et al (1998) The dependence of the electrical conductivity measured by time domain reflectometry on the water content of a sand. *Water Resour Res* 34(5):1207–1213
- Grysinski T, Moron Z (2011) Planar sensors for local conductivity measurements in biological objects-design, modelling, sensitivity maps. *Sensors Actuators B Chem* 158(1):190–198
- Han L, Liu S, Du Y (2006) New method for testing contaminated oil-electrical resistivity method. *Chi J Geotech Eng* 28(8):1028–1032
- Islam T, Chik Z, Mustafa M et al (2012) Modeling of electrical resistivity and maximum dry density in soil compaction measurement. *Environ Earth Sci* 67(67):1299–1305
- Kibria G, Hossain M (2012) Investigation of geotechnical parameters affecting electrical resistivity of compacted clays. *J Geotech Geoenviron Eng* 138(12):1520–1529
- Lee J, Shang J, Lee J et al (2011) Influencing factors on electrical conductivity of compacted kaolin clay. *Geomech Eng* 3(2):131–151
- Liu G, Wang Z, Huang J (2004) Research on electrical resistivity feature of soil and its application. *Chin J Geotech Eng* 26(1):83–87
- Moron Z (2003) Investigations of van der Pauw method applied for measuring electrical conductivity of electrolyte solutions: measurement of electrolytic conductivity. *Measurement* 33(3):281–290
- Muno-zcastelblanco J, Pereira J, Delage P et al (2013) The influence of changes in water content on the electrical resistivity of a natural unsaturated loess. *Astm Geotech Test J* 35(12/13):1927–1934
- Nahlik J, Kasparkova I, Fitl P (2011) Study of quantitative influence of specimen defects on measurements of resistivity of thin films using van der Pauw method. *Measurement* 44(10):1968–1979
- Nahlik J, Kasparkova I, Fitl P (2013) Influence of non-ideal circumferential contacts on errors in the measurements of the resistivity of layers using the van der Pauw method. *Meas J Int Meas Confederation* 46(2):887–892
- Preis W (2015) Modelling of surface exchange reaction, oxygen diffusion, and conductivity relaxation of solid oxides: application to the van der Pauw method on disk-shaped specimens. *Comput Mater Sci* 103(6):237–243
- Rakorenko N, Korotchen T (2016) Impact of petroleum products on soil composition and physicochemical properties. *Earth Environ Sci* 33(1):012028
- Singh D (2004) Measuring soil electrical resistivity using a resistivity box and a resistivity probe. *Geotech Test J* 27(4):496–497
- Son Y, Oh M, Lee S (2009) Estimation of soil weathering degree using electrical resistivity. *Environ Earth Sci* 59(6):1319–1326
- Vander P (1958) Method of measuring specific resistivity and hall effect of disks of arbitrary shape. *Phil Res Rev* 13:1–9
- Wychowaniak D, Zawadzki L, Lech M (2015) Application of column tests and electrical resistivity methods for leachate transport monitoring. *Ann Wars Univ Life Sci Land Reclam* 47(3):237–247
- Yu X, Liu S (2004) Researches on application of electrical resistivity indices to the microstructure of expansive soils. *Chin J Geotech Eng* 26(3):393–396
- Zha F, Liu S, Du Y et al (2008) Quantitative research on microstructures of expansive soils during swelling using electrical resistivity measurements. *Chin J Geotech Eng* 30(12):1832–1839
- Zha F, Liu S, Du Y et al (2010) Prediction of matric suction of unsaturated soil based on electrical resistivity. *Rock Soil Mech* 3:1003–1008
- Zhou W, Lee M (2010) A detector for plant electrical conductivity based on four-electrode method. *Sens Lett* 8(1):122–127
- Zhou Z, Zheng L, Sun B (2009) Research on relationships between water content and resistivity of earthen ruin walls. *Chin J Rock Mech Eng* 28(S2):4054–4058
- Zhou M, Wang J, Cai L et al (2015) Laboratory investigations on factors affecting soil electrical resistivity and the measurement. *IEEE Trans Ind Appl* 51(6):5358–5365